INFORMATION TO USERS

This reproduction was made from a copy of a document sent to us for microfilming. While the most advanced technology has been used to photograph and reproduce this document, the quality of the reproduction is heavily dependent upon the quality of the material submitted.

The following explanation of techniques is provided to help clarify markings or notations which may appear on this reproduction.

1. The sign or "target" for pages apparently lacking from the document photographed is "Missing Page(s)". If it was possible to obtain the missing page(s) or section, they are spliced into the film along with adjacent pages. This may have necessitated cutting through an image and duplicating adjacent pages to assure complete continuity.

2. When an image on the film is obliterated with a round black mark, it is an indication of either blurred copy because of movement during exposure, duplicate copy, or copyrighted materials that should not have been filmed. For blurred pages, a good image of the page can be found in the adjacent frame. If copyrighted materials were deleted, a target note will appear listing the pages in the adjacent frame.

3. When a map, drawing or chart, etc., is part of the material being photographed, a definite method of "sectioning" the material has been followed. It is customary to begin filming at the upper left hand corner of a large sheet and to continue from left to right in equal sections with small overlaps. If necessary, sectioning is continued again—beginning below the first row and continuing on until complete.

4. For illustrations that cannot be satisfactorily reproduced by xerographic means, photographic prints can be purchased at additional cost and inserted into your xerographic copy. These prints are available upon request from the Dissertations Customer Services Department.

5. Some pages in any document may have indistinct print. In all cases the best available copy has been filmed.

University Microfilms International
300 N. Zeeb Road
Ann Arbor, MI 48106

Hostetler, Charles James

EQUILIBRIUM PROPERTIES OF SOME SILICATE MATERIALS: A THEORETICAL STUDY

The University of Arizona PH.D. 1982

EQUILIBRIUM PROPERTIES OF SOME SILICATE MATERIALS: A THEORETICAL STUDY

by

Charles James Hostetler

A Dissertation Submitted to the Faculty of the

DEPARTMENT OF PLANETARY SCIENCES

In Partial Fulfillment of the Requirements
For the Degree of

DOCTOR OF PHILOSOPHY

In the Graduate College

THE UNIVERSITY OF ARIZONA

1 9 8 2

THE UNIVERSITY OF ARIZONA
GRADUATE COLLEGE

As members of the Final Examination Committee, we certify that we have read the dissertation prepared by Charles James Hostetler

entitled Equilibrium Properties of Some Silicate Materials: A Theoretical Examination

and recommend that it be accepted as fulfilling the dissertation requirement for the Degree of Doctor of Philosophy.

	July 15, 1982 Date
Michael J. Drake	July 16, 1982 Date
	7/16/82 Date
W.B. Hubbard	7/16/82 Date
Michael Bonsfield	7/16/82 Date
Walter B. Miller	7/16/82

Final approval and acceptance of this dissertation is contingent upon the candidate's submission of the final copy of the dissertation to the Graduate College.

I hereby certify that I have read this dissertation prepared under my direction and recommend that it be accepted as fulfilling the dissertation requirement.

Michael J. Drake	July 16, 1982
Dissertation Director	Date

STATEMENT BY AUTHOR

This dissertation has been submitted in partial fulfillment of requirements for an advanced degree at the University of Arizona and is deposited in the University Library to be made available to borrowers under rules of the Library.

Brief quotations from this dissertation are allowable without special permission, provided that accurate acknowledgment of source is made. Requests for permission for extended quotation from or reproduction of this manuscript in whole or in part may be granted by the head of the major department or the Dean of the Graduate College when in his judgment the proposed use of the material is in the interests of scholarship. In all other instances, however, permission must be obtained from the author.

SIGNED: Charles James Hostetler

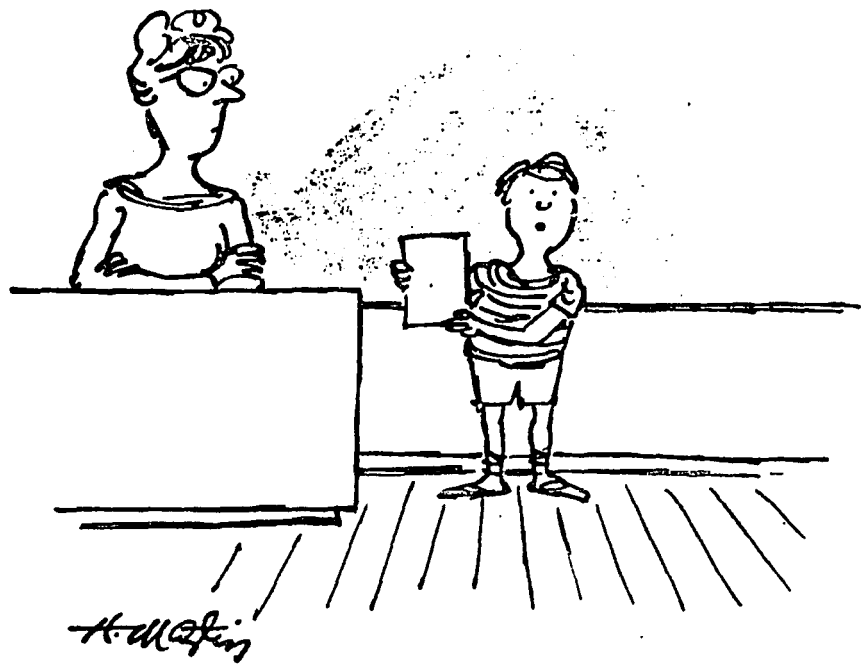

"I chose for my book report 'Excited States in Quantum Chemistry: Theoretical and Experimental Aspects of the Electronic Structure and Properties of the Excited States in Atoms, Molecules, and Solids.' Edited by Nicolaides and Beck. I didn't understand a word of it."

ACKNOWLEDGMENTS

I feel deep appreciation to Mike Drake for his support during the last four years. He was able to supply direction when necessary while still allowing me to work independently. Alex Woronow also aided the author greatly by generously spending many hours in deep discussion over almost every subject, occasionally including this dissertation. The Big A has been a constant haven for the past four years, and this dissertation could not have appeared without it. Finally I would like to thank Ann for her constant cheerfulness and support during the writing of this dissertation. I certainly appreciate it.

TABLE OF CONTENTS

LIST OF TABLES

LIST OF TABLES--Continued

LIST OF ILLUSTRATIONS

ABSTRACT

Equilibrium properties of the $MgO-Al_2O_3-SiO_2$ (MAS) system are modeled using techniques from statistical and quantum mechanics. The fundamental structural units in this model are the closed shell ions: Mg^{2+}, Al^{3+}, Si^{4+}, and O^{2-}. The equilibrium properties of the MAS system are determined by the interactions among these ions and by the environment (i.e. temperature and pressure). The interactions are modeled using coulombic, dispersion, and repulsive forces. Two parameters appearing in the repulsive terms for each cation-oxygen interaction are fitted from properties of quartz, corundum, and periclase crystals. The effects of the environment on the liquid and solid compositions found in this system are calculated using a Monte Carlo technique involving the generation of a Markov chain of configurations; each configuration being a "snapshot" of the particles in the liquid or solid material being studied. The properties of the material are derived from averaging appropriate quantities over all the configurations. Enthalpies of formation, heat capacities, and volumes of seven compositions in the MAS system have been calculated using this method. All are within three percent of the corresponding experimental values. Radial distribution functions for these runs show the competition among the cations for the common anion, oxygen, under charge and mass balance constraints.

The electronic structure of several molecular clusters in the MAS system are examined using ab initio linear combinations of atomic orbitals (LCAO) techniques. The assumptions used in LCAO calculations are examined and a small, balanced basis set for the MAS system is presented. The Mg-, Al-, and Si-O interactions are all found to be highly ionic using this basis set. Using a first principles technique, the two body effective pair potentials assumed for the Monte Carlo calculations were shown to be physically reasonable.

CHAPTER 1

INTRODUCTION

The crusts of the earth and moon consist primarily of solid silicate and oxide materials, many of which display their igneous origin. Compositions of the igneous rocks on both bodies differ in general from the bulk composition of the planet, evidence for the derivation of the igneous materials from various source regions via chemical differentiation. The wide diversity of igneous rocks on both the earth and the moon is exhibited in two fashions: the existence of separate, distinct rock associations and the variation in chemistry among rocks of each association. In order to explain the observed diversity of the igneous rocks Bowen (1928) postulated igneous differentiation as an important process in producing the solid silicate materials seen on the Earth.

An important goal of the igneous petrologist is the expression of the "laws" of igneous differentiation in mathematical form, based on physico-chemical theories. These "laws" simply describe the physical properties of silicate materials as a function of the surrounding environment, e.g. temperature and pressure. Naturally occurring silicate materials, both solid and liquid, are complex multicomponent solutions. The structural, thermodynamic, and transport properties of silicates reflect this complexity, and these

properties are in fact controlled entirely by the nature of the components of the material and by their interactions. (The word component is not used here in the strict thermodynamic sense, but rather as a general term for a fundamental structural and chemical unit.) A quantitative model for use with silicate materials describing a set of components and interaction laws, consistent with known data, and able to predict a wide variety of physical and chemical properties would be of general interest to the material sciences and of particular interest to igneous petrology.

Progress toward such an understanding has been difficult; and it seems the difficulty lies in identifying the nature of the components in the silicates and the fashion in which these fundamental structural units interact. Thermodynamic modelling produced some of the early insight into this problem. As Drake (1976) pointed out, thermodynamic models of silicate materials take one of two approaches: simple components which interact in a complex fashion, or complex components which interact in a simple fashion.

Examples of the former method are the predictions of multicomponent phase relations in terms of simple oxide components and stoichiometric mineral components by Bottinga and Richet (1978) and Barron (1972) respectively. Bottinga and Richet (1978) assumed excess free energies of mixing followed the van Laar and Flory-Huggins descriptions, while Barron (1972) described a general excess free energy model. Hostetler and Drake (1980) used the simple components/complex mixing concept in a statistical sense to correlate

major element chemistry with mineral/melt equilibria in basaltic systems. Using the complex components/simple mixing technique, multicomponent major element mineral/melt equilibria have been calculated for olivine/liquid pairs (Roeder and Emslie, 1970; Roeder, 1974; Longhi et al., 1978), plagioclase/liquid pairs (Drake, 1976), and pyroxene/melt pairs (Nielsen and Drake, 1979). Other examples of this method are the polymer model (Masson, 1968; Masson et al., 1970; Baes, 1970) and the ion-asociation model (Nesbitt and Fleet, 1981), used to predict activity/composition relations for binary MO-SiO_2 liquids (where MO is a metal oxide, e.g. CaO, MgO, FeO, PbO).

However, with respect to the goal of developing a general quantitative model for the structural, transport, and equilibrium properties of silicates, problems arise common to all thermodynamically based techniques. Each particular set of components, or mixing laws, is generally useful for only one or two systems, e.g. the simple oxide components in Roeder and Emslie's (1970) work on olivine/melt equilibria are not useful for explaining plagioclase/melt equilibria (Drake, 1976), and the polymer model has not been successfully applied to multicomponent systems (Fraser, 1977). The compositional range of applicability of these models is narrow, and usually cannot be extended. Of course these models are useful in their ability to predict some of the thermodynamic properties of silicates, but they are basically interpolation tools provising minimal information about the properties of silicates at the microlevel. When such information is implied, it is in terms of

adjustable parameters (usually equilibrium constants) chosen to fit a particular thermodynamic data set. Since the thermodynamic properties of any system are independent of the particular chemical entities we choose to use as thermodynamic components, the agreement of any model built purely on thermodynamic data with the same thermodynamic data cannot be regarded as proof (or strong confirmation) of the validity of that model in any structural sense. Such models do not predict or explain the structural and transport properties of silicate systems. For example, the polymer model and the ion-association model each independently fit the same activity/composition data in the $PbO-SiO_2$ system with different adjustable equilibrium constants. To make structural interpretations based on the success of either one of these models, e.g. that polymeric or ionic complexes actually exist in these silicate liquids, would be invalid (and in this example mutually inconsistent).

Experimental studies of some physical properties have led petrologists to some general conclusions about the nature of silicate materials at the molecular level. X-ray diffraction studies have shown that silicon is in tetrahedral coordination with oxygen in all silicate solids and liquids examined (Waseda, 1980). Electrical conduction in silicate liquids is primarily by mass transfer of ions, and is unipolar with mobile cations and fixed anions (Bockris et al., 1952a, 1952b; Bockris and Mellors, 1956). Negative deviations in the volumes of mixing along metal oxide-silica joins are evidence that cations have energetically favorable sites in broken down silica

networks (Bockris et al., 1956). Infrared vibrational spectra (McMillan, 1981) can be interpreted in terms of a model in which cations compete for oxygen, forming the strongest associations possible under mass and charge balance constraints. Unfortunately, no quantitative model which can predict this variety of silicate properties has arisen from such qualitative observations.

Theoretical examinations of the behavior of various small isolated silicate fragments have been made using several quantum mechanical methods (see DeJong and Brown, 1980 for references), but these results have not been connected with quantitative component/interaction models for reasons listed in Chapter 4. Prediction of most physical properties requires accurate calculation of potential energy as a function of geometry of the fragment. Semiempirical quantum mechanical techniques (e.g. DeJong and Brown, 1980) and the modified electron gas model (Tossell, 1980) have been applied to silicate materials without much success.

In order to calculate accurate binding energies, ab initio linear combination of atomic orbital (LCAO) calculations, which evaluate the energy of a system from first principles, previously required large basis sets (i.e. many mathematical functions per orbital) with high angular momentum orbitals attached to heavy atoms in the fragment (Carsky, 1980). The large amounts of computer storage and time required for these LCAO calculations severely limited the number of atoms in a fragment and the number of geometries studied for each fragment. Because the basis sets used in all published LCAO

calculations were optimized for neutral atoms instead of closed shell ions and the basis sets were of unequal size for different atomic centers, the counterpoise error and the correlation error (both spurious lowerings of potential energy due to the LCAO approximations) were of the same order of magnitude as the binding energy itself. Thus accurate first principles calculation of the properties of silicate materials has not been considered feasable.

The goal of this dissertation is the generation of a successful component/interaction model for silicate systems using fundamental principles of physical chemistry. Interaction potential functions for a simple set of components are calculated from lattice energy considerations for simple crystalline compounds. Use of these interaction potential functions with Ewald and Monte Carlo techniques allows calculation of a wide variety of physical and chemical properties of silicate solids and liquids. In addition, ab initio quantum mechanical calculations with an ion-optimised basis set determine from first principles the potential energy of various molecular clusters as a function of the positions of their constituent ions. The quantitative agreement of the potential models with experimentally derived observations of various physical properties provides a test of the validity of these models.

In the next chapter I discuss in detail the experimentally derived constraints mentioned above and consider various possible choices for components and interaction laws. That chapter also contains a description of the Monte Carlo method of obtaining physical

properties from interaction potential functions. Chapter 3 contains the results of Monte Carlo calculations for some compositions in the $MgO-Al_2O_3-SiO_2$ (MAS) system, a simple analog system exhibiting many of the features of more complicated geochemical systems: features which any successful model should correctly describe. Chapter 4 contains the results of quantum mechanical calculations for some small clusters found in the MAS system. A summary of the proposed structural model for general silicate systems as well as areas of possible future research are detailed in Chapter 5.

CHAPTER 2

COMPONENT/INTERACTION MODEL FOR SILICATE MATERIALS

The fundamental structural components and the nature of their interactions determine the physical and chemical properties of any system. In this chapter I first discuss several proposals for the nature of the basic structural and chemical units from which silicate materials are constructed. Second, I consider the development of interaction potential functions using both lattice energy considerations and statistical analysis of quantum mechanical data. Lastly I derive equations for the equilibrium properties of crystals and liquids from the interaction potentials.

Components

Several sets of structural components proposed in the literature include: the network-former/network-modifier theory (Bottinga and Weill, 1972), the polymer model and its extensions (Masson, 1968; Masson et al., 1970; Baes, 1970), an ion association model (Nesbitt and Fleet, 1981), and an ion competition model (McMillan, 1981). These theories were all advanced to explain the physical or chemical properties of selected sytems. The first three are deficient with respect to applicability to general silicate systems, and the fourth has not been developed into a quantitative model as yet. All are discussed in more detail below.

Bottinga and Weill (1972) developed a structural model to predict the viscosities of anhydrous silicate liquids using a linear regression approach. They found that a model based on network-forming and network-modifying components (see Table 1) was in best agreement with their data set. Note that these components are neutral oxides and multiple oxides. Drake (1976) and Nielsen and Drake (1979) used network-former/network-modifier theory to correlate plagioclase and pyroxene melt equilibria as well. However, Hostetler and Drake (1980) found that network-former/network-modifier theory could not be used to predict general major element mineral/melt equilibria in anhydrous basaltic systems.

Electrical conductivity studies of liquid silicates have shown that charge transfer in silicate liquids is by mass transfer of ions with mobile cations and relatively fixed anions (Bockris et al., 1952a, 1952b; Bockris and Mellors, 1956; Segers et al., 1978). Other measurements of liquid silicates indicate that with the addition of various oxides to silica large decreases in viscosity occur, indicating that the silica network is being broken down to produce fragments of various molecular weights (Bockris and Lowe, 1954; Bockris et.al., 1955; Riebling, 1964, 1966). Density data for liquid silicates show negative deviations from ideal volumes of mixing along metal oxide-silica joins (Bockris et al., 1956; Tomlinson et al., 1958; Henderson et al. 1961; Gaskell and Ward, 1967). These deviations were attributed to dissociation of metal oxide into a cation and a free oxygen anion. The anion is incorporated into the

Table 1

Bottinga/Weill (1972) Melt Components

Network Formers	Network Modifiers
SiO_2	FeO
$KAlO_2$	MgO
$NaAlO_2$	CaO
$CaAl_2O_4$	$NaO_{0.5}$
$MgAl_2O_4$	$KO_{0.5}$
$FeAl_2O_4$	

silicon-oxygen network, while the cations sit in sites between the fragments. This explanation is consistent with the widely held view that silicate crystals consist of cations occupying sites created by a silicon-oxygen framework (Eitel, 1954; Philpotts, 1978). Both of these observations seem to indicate that the Bottinga and Weill (1972) components are not present as discrete structural components in silicate materials; rather they are a convenient shorthand device for conceptualizing the above observations.

The above, along with the conclusion from x-ray diffraction data indicating silicon is always present in tetrahedral coordination with oxygen in silicates (Waseda, 1980), form the basis of the polymer model (and its extension) for silicate liquids (Masson, 1968, 1970; Baes, 1970). Table 2 lists the structural components in this model. The various structures of silicates are built up from silicon-oxygen tetrahedra in this model by condensation polymerization at the apices of the tetrahedra; the condensation product being a free oxygen anion. Chain, sheet, and framework structures can all be constructed in this way. Metal cations form the other basic structural unit. The free oygen anions and the metal cations occupy sites created by the silicon-oxygen lattice. While polymer theory has never been extended to geochemically relevant systems (Fraser, 1977 discusses the problems with the extension of polymer theory to multi-oxide systems) the structural units proposed are qualitatively consistent with most of the observed physical properties of silicates, and thus serve as a useful paradigm.

Table 2

Polymer Model Melt Components

Component	Explanation
M^{+}, M^{2+}, M^{3+}	Cation with high coordination numbers
T^{4+}	Cation in tetrahedral coordination with oxygen
O^{2-}	Oxygen anion
$T_n O_m^{K-}$	Polymer of order n,m built from tetrahedrally coordinated cations

The polymer model is, however, deficient as a structural model in several respects. The geometry of the tetrahedral unit itself is observed to vary with chemical composition, pressure, and temperature in crystals and liquids (Papike and Cameron, 1976; Waseda, 1980). Since the activation energies for diffusion of tetrahedrally coordinated silicon and aluminum in alkali feldspars are proportional to the site energies for these ions in feldspar crystals, Dowty (1980) suggested that tetrahedrally coordinated ions do not remain associated with the same four oxygen ions for indefinitely long periods of time. Oxygen is found as two different structural types in the polymer model: as part of tetrahedral units (either shared or unshared) and as free oxygen anions. These considerations seem to argue against the polymer model components as the simplest complete structural set.

Nesbitt and Fleet (1981) proposed that in lead oxide-silica melts the thermodynamic components PbO (l) and SiO_2 (l) associate to form a lead complex Pb_2SiO_4 (l). They assumed these thermodynamic components mix ideally in the liquid, and fitted an equilibrium constant for the association reaction to activity/composition data. The agreement between the activity/composition data and their regression equation (containing the constant fitted to the data) led Nesbitt and Fleet tc believe that lead orthosilicate is the predominant species in lead oxide-silica melts. Even if this conclusion is correct for lead oxide-silica melts, it does not hold for other metal oxide-silica binary liquids or for multioxide liquids in general. The polydisperse nature of liquid silicates has been

shown experimentally with chromatographic methods (Lentz, 1963; Gotz and Masson, 1971) and x-ray diffraction (Waseda, 1980).

McMillan (1981) proposed an ion competition scheme based on his interpretation of infrared Raman spectra for the systems $CaO-MgO-SiO_2$ and $CaO-Al_2O_3-SiO_2$. He inferred a stronger oxygen interaction for silicon than for magnesium, calcium, or aluminum, and emphasized the stability of the SiO_4 tetrahedral unit. However, McMillan also stressed the competition of aluminum for oxygen, and ranked the relative strengths of the other cation interactions with oxygen: $Ca^{2+} < Mg^{2+} < Al^{3+} < Si^{4+}$. McMillan was unable to make any inferences from his spectra about the nature (e.g. the degree of covalency or absolute strength) of the cation-oxygen interactions. Indeed, it is perhaps a misnomer to label the particles in McMillan's model "ions" since he was also unable to infer their charges.

Individual particles are certainly a very simple set of components. A modification of the ion-competition model will serve as the basis for the work in this dissertation. In this modification, the components are taken as the closed shell ions. (Transition metal elements may exhibit several valance states in this scheme, for example Fe^{2+} and Fe^{3+}.) These closed shell ions each have an effective charge varying as a function of the surrounding chemical and physical environment, but the interactions among ions are essentially coulombic with a repulsive core. Of course, all silicate structures can be built up from these simple ionic components.

This ion competition model is in qualitative agreement with the known coordination properties of ions in silicate materials. We can imagine a set of these particles occupying some fixed volume, but allowed to arrange themselves to seek their minimum potential energy positions. We define a quantity-- the cation reference potential-- as the coulombic potential energy a closed shell cation and an oxygen anion would have if separated by the sum of their ionic radii. Such a quantity measures how strongly a particular cation competes for the common anion, oxygen. Table 3 is a list of some common cations in silicates and their cation reference potentials. As can easily be seen, silicon has the most negative potential, and thus is always able to capture the four oxygens it requires to satisfy its coordination sphere. Titanium has the second most negative potential, and depending on the amount of oxygen available in the system, enters partially or entirely into tetrahedral coordination. If any oxygen is left over, it forms strong complexes with aluminum, then Fe^{3+}, and so on until all the oxygen is used up. Cations with small potentials are unable to form strong associations with oxygen, and are left to distribute themselves around the lattice in various sites to help satisfy charge balance and packing constraints, as in the polymer model.

Potential energy functions are needed to transform these qualitative ideas into a quantitative model. In the next section I will discuss the generation of the required potential energy functions using both an empirical lattice-energy based technique and a quantum

Table 3

Cation Reference Potentials

Cation	Potential
Si^{4+}	-4.42
Ti^{4+}	-3.48
Al^{3+}	-3.16
Fe^{3+}	-2.78
Mg^{2+}	-1.95
Fe^{2+}	-1.85
Ca^{2+}	-1.67
Na^{+}	-0.85
K^{+}	-0.73

mechanical technique. Although there is abundant evidence that bonding in silicates is at least partly ionic (see above) the effective charges (and thus the degree of ionicity) for the ionic components are not known. The quantum mechanical technique used to obtain the interaction potential functions allows calculation of the effective charges on each on the ions in a cluster. This method is also discussed in the next section.

Interaction Potential Functions

The interactions of the cations with oxygen are actually more complicated than considered above in the discussion of the ion competition model. Contributions from other than the strict coulombic term must be included in any detailed quantitative model. In particular, a repulsive term must be included to keep the system from collapsing into zero volume. Terms representing other interactions may also be included. I now take up a general discussion of interparticle interactions.

Consider a system of N interacting particles. The total potential energy of this system is given by:

$$U = \frac{1}{2!} \sum_{\substack{i=1 \\ i\neq j}}^{N} \sum_{j=1}^{N} \phi_{ij} + \frac{1}{3!} \sum_{\substack{i=1 \\ i\neq j\neq k}}^{N} \sum_{j=1}^{N} \sum_{k=1}^{N} \phi_{ijk} + \cdots \qquad (2.1)$$

relative to a standard state of infinitely dispersed ions. The summands are the two- and three-body interation potentials. In lieu of adequate theoretical knowledge of the effects of many-body interactions, defining an effective pair potential which is pairwise

additive and reproduces the potential energy of the system is convenient:

$$U = \left\langle \frac{1}{2} \sum_{i=1}^{N} \sum_{j=1}^{N} \phi_{ij}^{eff} \right\rangle \tag{2.2}$$

where the angular brackets denote an ensemble average. The degree to which the effective pair potential fails to predict other properties of the system is a measure of the importance of many-body interactions. On the other hand, agreement between an effective pair potential model and measured equilibrium properties does not imply that two-body interactions are the only quantitatively important interactions. (I will discuss this subject again with specific reference to silicate systems in Chapter 4.)

Interaction functions can be determined either empirically or from first principles. The empirical technique relies on finding adjustable parameters in an interaction function by examining the total internal energy and its derivatives with respect to volume for a crystal. Usually three equations are used:

$$U(\underset{\sim}{r}_0) = U_0 \tag{2.3}$$

$$\left.\frac{dU}{dr}\right|_{\underset{\sim}{r}_0} = 0 \tag{2.4}$$

$$\left.\frac{d^2U}{dr^2}\right|_{\underset{\sim}{r}_0} = \frac{9V}{\kappa} \tag{2.5}$$

where r_0 represents the equilibrium geometry, U_0 is the potential

energy at the equilibrium geometry, V is the volume, and κ is the isothermal compressibility of the crystal. Thus three parameters can be fit. A variation on this method is to fit for two parameters (most analytic potential functions contain two parameters) and use one of the three equations above as a check for consistency. Either of these variations has the advantage of generating accurate fits for energy and geometry very quickly and inexpensively.

Tosi and Fumi (1964) showed that a potential function following the Born model of an ionic solid (Born and Mayer, 1932) with the generalized Huggins-Mayer form for the repulsive interaction (Huggins and Mayer, 1933; Huggins, 1937, 1947) correctly matched some crystalline data for NaCl-type alkali halides. This potential has the form:

$$\phi_{ij}(r) = \frac{Z_i Z_j e^2}{r} + \frac{C_{ij}}{r^6} + \frac{d_{ij}}{r^8} + Aexp(-Br) \qquad (2.6)$$

where the Z_i are formal ionic charges, e is the fundamental unit of electronic charge, c_{ij} and d_{ij} are constants related to the dispersion potential (Ladd, 1974; Hirschfelder et al., 1954), and A and B are adjustable constants fit to crystalline data, using equations (2.3), (2.4), and (2.5). The terms in this expression represent coulombic, dispersion (2 terms) and repulsive potential energy contributions respectively. This potential energy function represents rigid-ion interactions, and has been employed extensively for alkali halide

systems (e.g. Woodcock and Singer, 1971; Adams and McDonald, 1974; Lantelme et al., 1974).

Pauling (1928) used a function of the form:

$$\phi_{ij}(r) = \frac{Z_i Z_j e^2}{r} + \frac{C_{ij}}{r^6} + \frac{d_{ij}}{r^8} + Ar^{-B} \qquad (2.7)$$

to represent interactions in various systems. The only difference between (2.6) and (2.7) lies in the form of the repulsive term. Note that the Pauling form for the repulsive interaction has an analytic singularity at r=0, while an artificial singularity has to be introduced into the Tosi and Fumi form. The parameters A and B are determined using the method described above. Again, this interaction potential was derived to represent the interactions between rigid ions.

The first principles quantum mechanical technique relies upon finding the interaction energy of a system as a function of geometry:

$$\sum_i \sum_j \phi_{ij}(\underset{\sim}{r}) = E_C - \sum_i E_i \qquad (2.8)$$

where r_i is the position of the i^{th} particle, E_C is the energy of the cluster, and E_i is the energy of particle i. Swaminathan et al. (1977) describe a method for determining interaction potential functions for use in (2.1) and (2.2) from a data set consisting of geometries and interaction energies calculated from quantum mechanics. This method relies on fitting disposable parameters in an analytic potential function (APF) using the least-squares technique. The APF

is generally chosen with a physical model in mind; however, some APF's are chosen for their generality or mathematical convenience.

After the interaction potential functions have been determined, either by empirical or first principles methods, they are used to find the potential energy of a system as a function of geometry with (2.1). However, there are other properties of interest, and a method is needed to calculate properties for extended systems, i.e. liquids and crystals. Such a method is the subject of the next section.

Properties of Extended Systems

The first difficulty in obtaining the properties of extended systems from interaction potentials lies in the nature of the long-range coulombic term. For both liquid and crystalline systems a method for dealing with the conditional convergence of this term has been developed by Ewald (1921). The particles are placed in a basic cell (which may correspond to the unit cell for a crystalline system) and the cell is "expanded" through the use of periodic boundary conditions. For crystals this periodic cell must have the symmetry of the crystal itself. For liquids the cell is cubic, and as many particles as computationally feasable are included in the basic cell to minimize periodicity and edge effects. Useful expressions for the coulombic potential energy of such systems were given by Tosi (1964). Once the coulombic term is dealt with, the evaluation of other properties is straightforward, as discussed below.

Crystals

In this section I derive some of the equilibrium properties of perfect crystals at $0^{\circ}K$. The potential energy of the system is obtained as described in the previous section, along with lattice sums for the terms other than the coulomb term (Tosi, 1964). The internal energy is:

$$E = \langle U \rangle + \frac{3}{2} NkT \qquad (2.9)$$

where the second term on the right side is the kinetic energy of the system. The brackets denote an ensemble average. The enthalpy of the system is:

$$H = \langle E + pV \rangle \qquad (2.10)$$

where p is the pressure and V is the volume. The volume of the system can be found by minimizing the enthalpy with respect to volume at a given pressure.

Liquids

The terms other than the coulomb term in the potential energy are evaluated using the minimum image convention (Brush et al., 1966) in the basic cell. However, a Monte Carlo technique is also required to evaluate the properties of disordered materials. The Monte Carlo method is used in constant pressure form to facilitate comparison with experiment.

The isobaric-isothermal (N,p,T) ensemble represents a system of N particles with a specified temperature T and pressure p. The

cell length, i.e. volume of the system is variable. The Monte Carlo method for this ensemble was first described by Wood (1968). Starting from a given initial configuration, a Markov chain of configurations is generated by randomly choosing a particle and displacing it from its previous position by a random amount. The volume of the system is also changed a random amount. The energy of each configuration is calculated using equation (2.1). If the change in the quantity (U'-U)+p(V'-V)/kT for the transition from a state with potential energy U and volume V to a state U' and V' is negative the configuration is accepted for inclusion in the ensemble average with unit probability. Otherwise the configuration is accepted for inclusion with probability equal to the transition probability, which is just exp(-((U'-U)+p(V'-V))/kT), (where k is Boltzmann's constant). If the configuration is rejected (with probability=1-transition probability) the old configuration is retained and included in the ensemble average. Thus each configuration shows up in the ensemble average with frequecy proportional to its Boltzmann weighting factor. The process is repeated for the number of configurations desired.

The initial configuration can either be a crystalline lattice or a configuration in which the positions were chosen at random. If the system is not initially in its equilibrium state, it relaxes to equilibrium as the Markov chain proceeds. The rate at which the system approaches equilibrium is governed by two jump parameters: the maximum displacement of any particle and the maximum change in the volume for a jump. The sampling efficiency and accuracy of the

ensemble averages depend on these parameters, which must be chosen carefully for each application. These parameters are usually chosen such that the ratio of accepted configurations to rejected configurations is unity. The number of configurations the system takes to relax may not be small compared to the total number of configurations that can be made during a run, so in these cases the initial portion of the chain is not included in the averaging.

The average of any configuration-dependent property over all included configurations corresponds to the average of the property in the (N,p,T) ensemble. In particular, the internal energy and the enthalpy are found using (2.9) and (2.10). The volume is simply the ensemble average of the volumes of each of the configurations. Results from a (N,p,T) ensemble average can be directly compared to constant temperature-pressure experiments. An additional feature of the Monte Carlo technique is that it can be used to examine the properties of solids at temperatures other than $0^{\circ}K$, as well as solids with lattice defects.

In the next chapter, I will discuss some of the results of potential function, lattice, and Monte Carlo calculations for the MgO-Al_2O_3-SiO_2 system. This analogue system exhibits most of the diverse properties of natural geochemical systems. In Chapter 4 I will discuss the results of quantum calculations for the same system, and compare the resulting potentials with the empirically derived potentials.

CHAPTER 3

IONIC MODELS FOR THE $MgO-Al_2O_3-SiO_2$ SYSTEM: EMPIRICAL POTENTIAL FUNCTIONS

Chapter 2 contains equations for the equilibrium properties of a system given the interaction potential functions for the system. In Chapter 3 I first consider several empirical potential functions for the $MgO-Al_2O_3-SiO_2$ (MAS) system. Some of the equilibrium properties for several compositions in this system are calculated using the Monte Carlo technque. The MAS system is a simple basaltic analogue system with many of the features of more complicated natural petrologic systems.

Ionic Potential Models

Generation of empirical interaction potentials was discussed in Chapter 2. I consider both the Pauling (1928) (Equation 2.6) and exponential (Tosi and Fumi, 1964) (Equation 2.7) forms for the repulsive term. Both contain two parameters; I used equations 2.3 and 2.4 as constraints to determine these parameters, and 2.5 as a consistency check. The dispersion coefficients (c_{ij} and d_{ij} in Equations 2.6 and 2.7) were determined using the method of Ladd (1974), and are listed in Table 4. The data for the three crystalline phases (periclase, corundum, and β-quartz) used to determine the parameters are listed in Table 5. (For the tables in this chapter, unless otherwise mentioned, the uncertainties in quoted values are in

Table 4

Dispersion coefficients for the MAS system

c_{ij} ($\times 10^{-60}$ erg cm^6)

	O	Mg	Al	Si
O	44.4			
Mg	9.87	7.02		
Al	4.89	4.05	2.44	
Si	2.68	2.46	1.53	0.982

d_{ij} ($\times 10^{-76}$ erg cm^8)

	O	Mg	Al	Si
O	41.9			
Mg	10.2	7.91		
Al	4.10	3.93	1.98	
Si	2.08	2.13	1.09	0.597

Table 5

Properties of periclase, corundum, and β quartz at $0^{o}K$

		periclase	corundum	β quartz
$\Delta H^{0}_{f,0}$ [a]	(kJ/mol)	-597.3	-1663.7	-906.1
U_0 [b]	(kJ/mol)	-3884.5	-15446.8	-13205.6
U_C [c]	(kJ/mol)	-4611.9	-18108.1	-15167.6
U_V [d]	(kJ/mol)	16420.4	57891.1	7576.7
U_6 [e]	(kJ/mol)	-77.0	-146.0	-85.9
U_8 [e]	(kJ/mol)	-12.9	-25.8	-17.5
V [f]	(cm^3)	11.248	25.575	22.688

a. JANAF (1971).
b. Binding energy, Tosi (1964), Wackmann et al.(1967).
c. Coulomb energy, Madelung constants from Johnson and Templeton (1961).
d. Volume energy, Clark (1966).
e. Dispersion energies, This work.
f. Robie et al. (1978).

the last decimal place.) The term labeled volume energy is just the right hand side of (2.5). The repulsive energy is the difference between the binding energy and the coulomb and dispersion energies. The volumes given by Robie et al. (1978) are for 298°K, and the correction factor to 0°K is unknown, but given reasonable values for the thermal expansivity, these correction factors should be small. This approximation contributes less than 1 kilojoule error in the calculated energies. The parameters derived for both the Pauling and exponential repulsive terms are listed in Table 6 for the Si-O, the Al-O, and the Mg-O interactions.

In both of the interaction models all of the like-sign interactions (i.e. ++ and --) contain no contribution from the repulsive term. This should be a good approximation for the MAS system; because of the small size of the positively charged ions, and with the relatively large distance separating each anion pair the coulombic term dominates. In fact, for alkali halides, in both the Pauling and Tosi formalisms, repulsive interactions between cations account for less than 0.1 percent of the total energy (Adams and McDonald, 1974). Due to the large magnitude of the dispersion interaction between two oxygen anions (Table 4) the oxygen-oxygen interaction is more complicated (Figure 1). At small interparticle separations the dispersion term dominates and the total interaction energy (without a repulsion term) becomes negative. In actuality, the Pauli exclusion principle, manifested in repulsive energy, would keep two oxygen anions from approaching so closely. To correct for this,

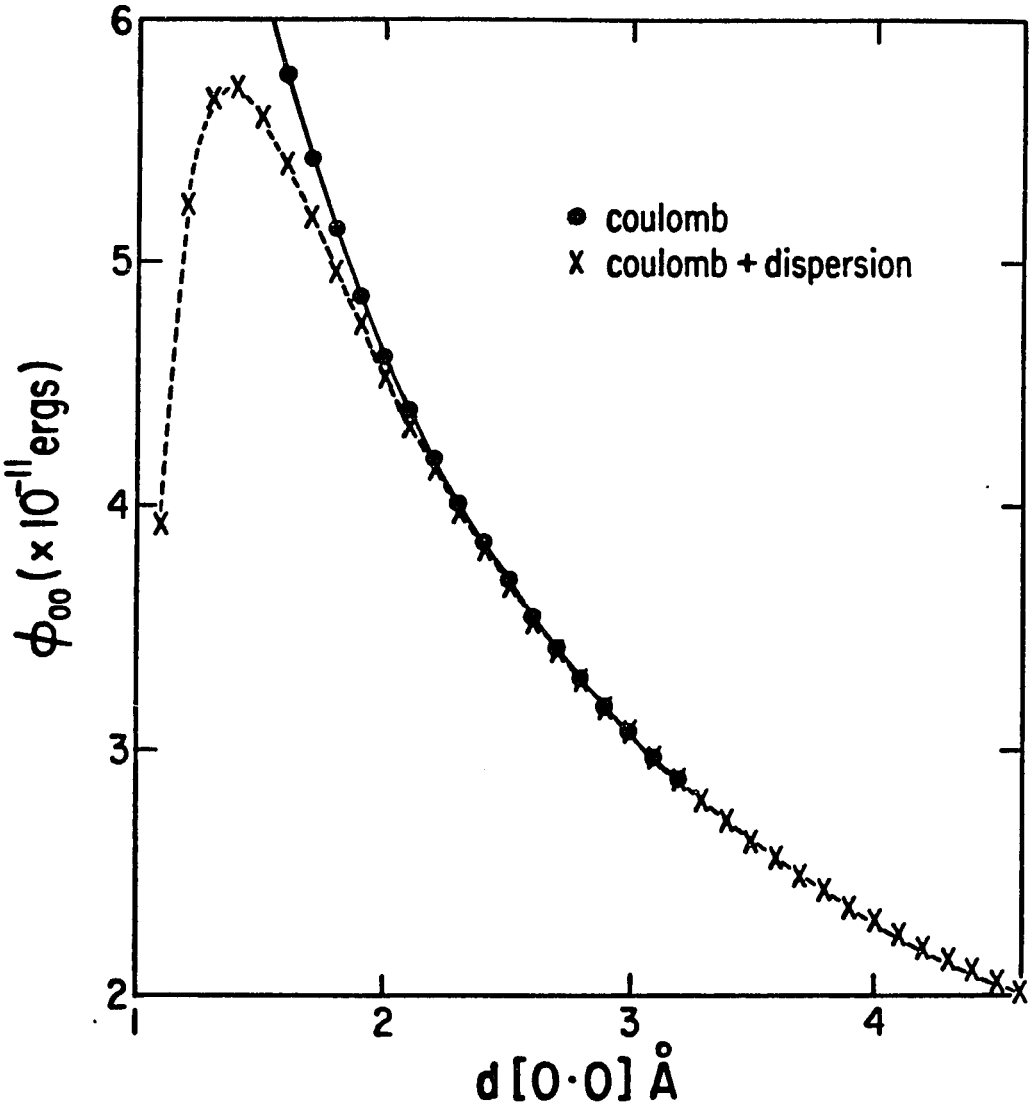

Figure 1. The Oxygen-Oxygen Interaction. -- At small interparticle separations the dispersion term dominates the total interaction energy. To correct for this effect without adding additional parameters, the potential used in this work follows the coulomb curve at distances less than 2.3 angstroms, and the coulomb+dispersion curve at distances greater than 2.3 angstroms.

without the addition of two more parameters for a repulsive term, the dispersion terms are "switched off" inside 2.2 angstroms and only the coulombic term is left. Since in silicate systems the oxygen-oxygen separation distance is usually 2.6 angstroms or greater the quantitative effects of this approximation are very small. Only the cation-oxygen interactions contain a repulsive term, which creates local minima in the cation-oxygen potential functions. The cation-oxygen potentials are shown in Figure 2.

The quantity in the last column in Table 6 is the ratio between the left and right hand sides in Equation 2.5. If either model were strictly valid for this system, the ratio would be unity. There is little quantitative difference between the ratios of the two models for each crystalline phase. Figure 3 shows the repulsive energy for a SiO_4^{4-} tetrahedron as calculated with both the Pauling and the exponential forms. As there is little difference between the Pauling and the exponential form in the region 1.6 to 1.7 angstroms, and the Pauling form is easier to use in Monte Carlo calculations, it will be used as the standard model for further calculations.

Thermodynamic Properties

Three low temperature (298°K) runs were made in the MAS system, one at each apex. These runs consist of 100,000 configurations each. The acceptance/rejection ratio ranged from 1.03 to 1.05, indcating that configuration space was adequately sampled. The runs were each started from the appropriate crystalline

Table 6

Parameters in the Pauling and exponential repulsive energy terms

Cation	form	a	b	ratio[a]
Si	Pauling $(\frac{a}{r^b})$	1.72185×10^{-71}	7.66099	3.20
	exponential (ae^{-br})	1.82106×10^{-8}	4.74953×10^{8}	2.83
Al	Pauling	2.68079×10^{-64}	6.77368	1.46
	exponential	3.42837×10^{-9}	3.4038×10^{-8}	1.27
Mg	Pauling	5.34867×10^{-61}	6.33439	1.27
	exponential	1.27490×10^{-9}	3.00778×10^{-8}	1.10

a. See text for explanation.

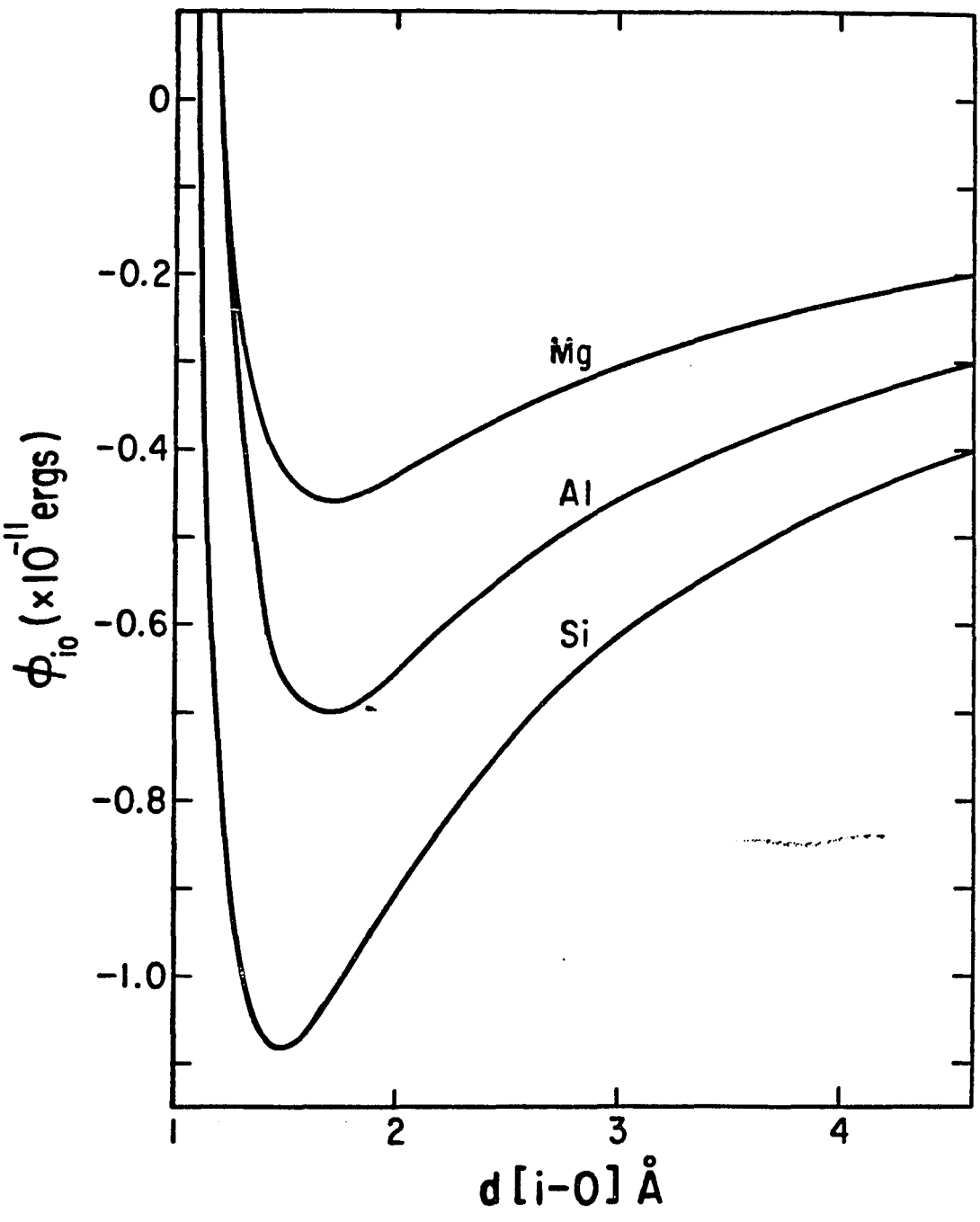

Figure 2. The Cation-Oxygen Interactions. -- The interaction potentials for i-O pairs, where i is magnesium, aluminum, or silicon, contain repulsive terms which create absolute minima.

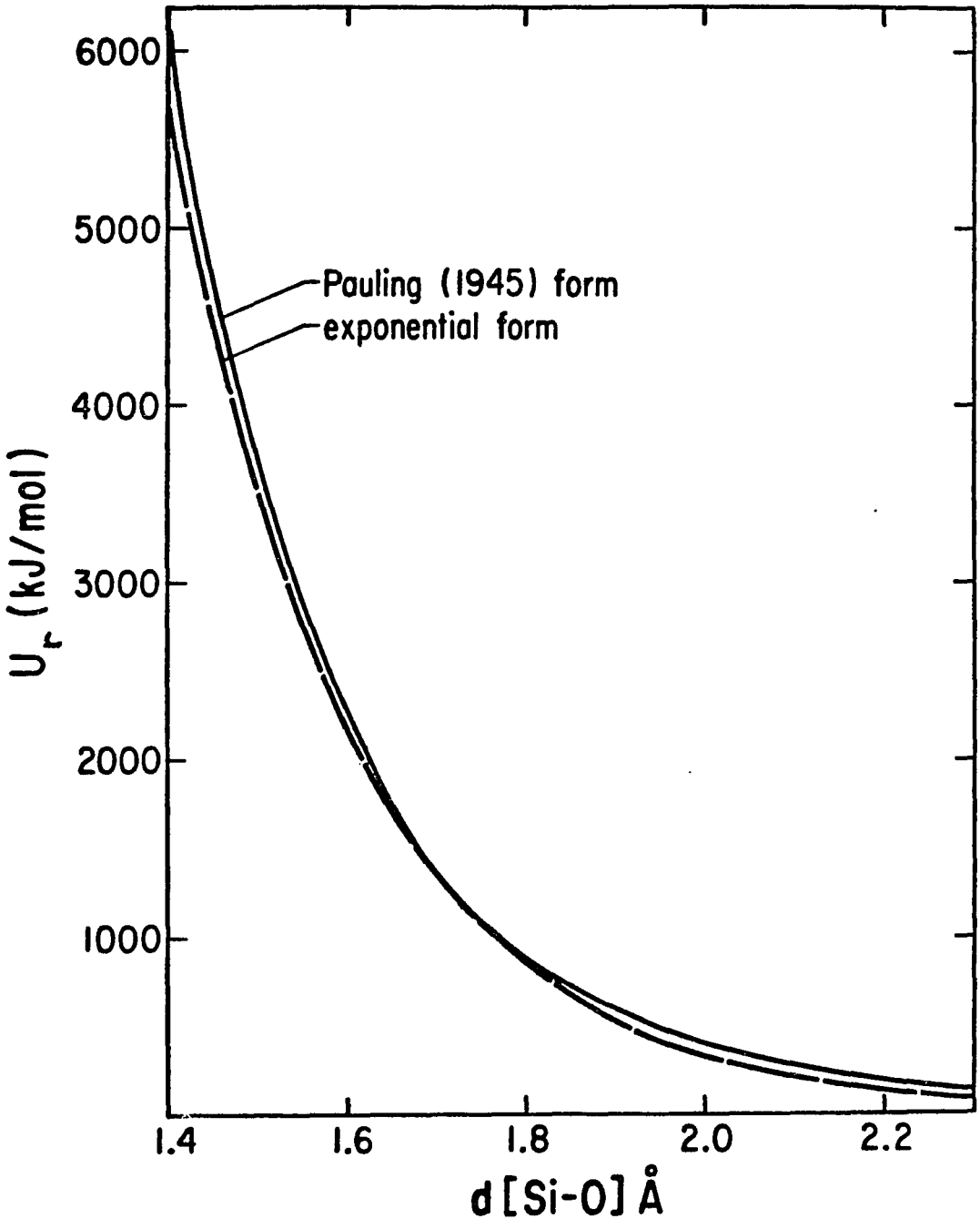

Figure 3. Repulsive Energy for the SiO_4^{4-} Tetrahedron. -- The one-atmosphere equilibrium Si-O distance is 1.61 angstroms. There is little quantitative difference between the two forms for the repulsive energy in this region.

configuration, and equilibrium was rapidly achieved. The first 20,000 configurations were discarded however, to ensure that the starting configuration did not influence the results.

The results from these runs are presented in Table 7. The heats of formation, heat capacities, and volumes all agree with experiment within one percent. The calculated volumes are systematically lower and the calculated energies are systematically more negative than the experimental values. This indicates that the potential well does not rise as steeply as it should inside the equilibrium point, i.e. the repulsive contribution to the energy is too small. This 1 to 5 kilojoule error is a consequence of the approximations mentioned above.

Seven high temperature ($2200^{\circ}K$) runs were also made in the MAS system. The runs at the MgO and Al_2O_3 corners were below the respective melting points, but the other runs were at least 75 above the liquidus. (The compositions of these runs are listed in Table 7.) The acceptance/rejection ratios ranged from 1.00 to 1.07. All of the runs except for the ternary composition were started from the appropriate crystalline configurations. The ternary run was started from a random configuration. Each run lasted 300,000 configurations with the first 50,000 configurations discarded. As in the low temperature runs, equilibrium was again attained rapidly, and configuration space was adequately sampled.

The results from these seven runs are also contained in Table 7. Again the agreement with experimental heats of formation and heat

Table 7

Monte Carlo Results for the MAS System

Composition	Temp(^{o}K)	ΔH_f^0 (kJ/mol)		C_p (J/mol K)		V (cm^3)	
		calc.	exp.[a]	calc.	exp.[a]	calc.	exp.[a]
M (s)	298	-602.5	-601.3	37.21	37.17	11.21	11.25
A (s)	298	-1681.0	-1675.4	79.18	79.08	25.51	25.58
S (s)	298	-904.1	-902.7	44.50	44.19	26.65	26.69
M (s)	2200	-728.2	-724.6	55.66	55.62	12.35	12.20
A (s)	2200	-1678.4	-1669.4	140.0	139.97	27.13	26.88
S (ℓ)	2200	-932.7	-931.2	85.79	85.78	27.20	27.22
M_2S (ℓ)	2200	-2390.7	-2376.6	210.13	205.03	17.22	-
MS (ℓ)	2200	-1661.9	-1628.8	147.44	146.45	19.77	19.64
AS (ℓ)	2200	-2513.1	-	246.82	-	27.10	-
$M_1A_1S_8$ (ℓ)	2200	-943.7	-	93.89	-	25.64	27.50

a. JANAF (1971).

b. Robie et al. (1978).

c. Riebling (1964) at 2000^{o}K.

capacities is good. The experimental results for the volumes for the high temperature runs are derived by interpolation from the results of Riebling (1964) at 2000°K. The volumes at 2200°K should actually be slightly larger. Again it can be seen from these results that the repulsive contribution to the pair potentials is not large enough at separations greater than the 0°K equilibrium value. Although the relative error is approximately the same as for the low temperature runs (less than 2 percent) the absolute error is much larger for the high temperature runs (5 to 10 kilojoules).

In order to further test the validity of the ion competition model, heats of mixing (Table 8) have been calculated from the results in Table 7. These quantities are much more sensitive to error because they are small differences between large numbers. Thermodynamic data from JANAF (1971) were used to convert to a liquid standard state at 2200°K where necessary for calculation of heats of mixing. The uncertainty assigned to the heats of mixing is 10 kilojoules. The heat of mixing for the orthosilicate composition is very close to the experimental value given the uncertainty in the quantities, although the metasilicate heat of mixing is too large by 28 kilojoules. The positive heat of mixing for the ternary compound, and the very low heat of mixing for the AS composition lend support to the speculation that liquid immiscibility is not confined to regions near the MS join, pinching out with the addition of alumina (Navrotsky et al., 1982).

Volumes of mixing have also been calculated for some compositions in the MAS system (Table 9). These quantities are upper

Table 8

Heats of mixing

	ΔH_{mixing}, 2200°K (KJ/mol)	
	calc. (±10.0)	exp.[a] (±10.0)
M_2S	-150.0	-144.6
MS	-75.2	-47.2
AS	-20.0	-
$M_1A_1S_8$	+23.9	$\overset{?}{>} 0$[b]

a. JANAF (1971).

b. Navrotsky et al. (1982).

Table 9

Volumes of Mixing

	ΔV_{mixing}, 2200°K(cm^3)	
	calc. (±0.03)	exp.[a] (±0.03)
M_2S	<-0.08	-
MS	<-0.065	<-0.07
AS	<-0.065	-
MAS_8	<-0.068	-

a. Seifert et al. (1982).

bounds on the true volumes of mixing due to the unknown volume change upon fusion of metastable alumina and MgO at 2200°K. The value for the magnesium orthosilicate is less than for the magnesium metasilicate, reflecting the competition for the oxygen anions between magnesium and silicon. The greater quantity of magnesium at the orthosilicate composition gives the magnesium cations a greater degree of control in determining the oxygen framework structure. Due to the large size of the magnesium cation, the silicon-oxygen framework is broken down, and the magnesium cations are admitted into the structure.

Radial Distribution Functions

Radial distribution functions have also been obtained from the Monte Carlo runs. The first nearest neighbor peak positions and populations for the MS join are given in Table 10. The experimental results are from the x-ray diffraction work of Waseda (1980). The 298 K results can be compared with the Si-O and O-O distances in β-quartz of 1.613 and 2.64 angstroms respectively. Although the volume calculated for this composition is lower than the experimental value, the individual tetrahedra are somewhat larger and the Si-O-Si intertetrahedral angle is lower than the experimental value. At high temperature the peak positions remain the same and the populations increase to near the ideal values.

With the addition of 50 mole percent MgO, the silicon-oxygen tetrahedra expand. The magnesium-oxygen distance is larger than the equivalent distance in periclase. These results, and similar results

Table 10

Radial distribution functions along the MS join

			r (Å)		N (atoms)	
			calc. (±0.02)	exp.[a]	calc. (±0.2)	exp.[a]
SiO_2	(298)	Si-O	1.63		3.9	
		O-O	2.66		5.8	
		Si-Si	3.17		3.6	
SiO_2	(2200)	Si-O	1.63	1.62	4.1	3.9
		O-O	2.66	2.63	6.0	5.7
		Si-Si	3.18	3.12	3.9	3.8
$MgSiO_3$	(2200)	Si-O	1.64	1.63	4.1	3.9
		Mg-O	2.12	2.16	4.6	4.8
		O-O	2.67	2.65	5.9	5.9
		Si-Si	3.20	3.16	3.9	3.7
Mg_2SiO_4	(2200)	Si-O	1.66		4.1	
		Mg-O	2.10		5.5	
		O-O	2.68		5.8	
		Si-Si	3.21		3.8	
MgO	(2200)	Mg-O	2.09	2.11	5.9	6.0
		O-O	2.96	2.98	7.8	8.0
		Mg-Mg	2.96	2.98	8.0	8.0

a. Waseda (1980).

Table 11

Radial distribution functions along the AS join

			r (Å)		N (atoms)	
			calc. (±0.02)	exp.[a]	calc. (±0.2)	exp.[a]
SiO_2	(2200)	Si-O	1.63	1.62	4.1	3.9
		O-O	2.66	2.65	6.0	5.7
		Si-Si	3.18	3.12	3.9	3.8
Al_2SiO_5	(2200)	Si-O	1.66		3.7	
		Al-O	1.75		3.9	
		Al-O	2.07		5.4	
		O-O	2.73		5.6	
Al_2O_3	(2200)	Al-O	1.93		5.6	
		O-O	2.55		5.7	
		Al-Al	2.70		5.1	

a. Waseda (1980).

for the orthosilicate composition imply that magnesium does indeed compete with silicon for the oxygen. This competition is also manifested by the change in magnesium-oxygen coordination from 4.6 at the metasilicate to 5.5 at the orthosilicate.

Table 11 lists the nearest neighbor positions and populations for compositions along the AS join. The silica peaks are as described before, while the alumina peaks compare closely with the structure of corundum. However the behavior at the aluminum metasilicate composition is more complicated. Silicon-oxygen coordination is less than four-fold, and the Si-O distance has increased significantly. The Al-O distribution function shows two large, ill resolved peaks. The population of the peak at 1.75 angstroms indicates that aluminum competes strongly enough for oxygen to achieve four fold coordination at this composition. The peak at 2.07 angstroms has a non-integral coordination number consistent with the suggestion of McMillan and Piriou (1982) that aluminum assumes a variety of coordination numbers at high alumina contents.

The ability of the quantitative ion-competition model to accurately calculate thermodynamic and structural properties of silicate materials is established by the results presented in this chapter. These results lend support to the picture of silicate materials as a sea of cations competing for oxygen anions, and trying to keep the cation-cation and oxygen-oxygen distances as large as possible. Of course the temperature and pressure, as well as mass and charge balance constraints, influence the structure and thermodynmic

properties of the system. In the next chapter the electronic structure of several silicon-, aluminum-, and magnesium-oxygen clusters will be examined using first principles quantum mechanical methods. The charge distribution and degree of ionicity in these cluster will be determined, and interaction functions will be developed and compared with the potentials obtained in this chapter.

CHAPTER 4

QUANTUM MECHANICAL INVESTIGATIONS OF SILICATES

In Chapter 3 I derived a set of interaction functions which describe the potential energy of a system (in $MgO-Al_2O_3-SiO_2$, MAS) as a function of the positions of the particles in the system. These potentials were calculated using the method described in Chapter 2, with the heats of formation and the isothermal compressibility for crystals in MAS as input data. In this chapter I present a set of first principles calculations of the energies of several small clusters in the MAS system for comparison with the empirical potential functions described above.

Ab initio quantum mechanical calculations methods involve computing all necessary one- and two-electron integrals; after certain initial assumptions are made (discussed below and in Chapter 5), no input data are needed to evaluate the expectation value of the Hamiltonian, and thus the energy of the system. This is in contrast with "semi-empirical" techniques in which certain integrals are approximated with constants adjusted to fit thermodynamic data. In principle, given sufficient computer time, the equilibrium properties of a given system could be derived entirely from first principles, using ab initio calculations to determine interaction potentials for the system, in conjunction with the Monte Carlo method described in

Chapter 2. In practice this is impractical given present limitations on computer storage and time.

The results of the ab initio calculations will be compared with the empirical potential functions derived in Chapter 2 in order to obtain more information about the potential energy as a function of geometry in the MAS system. One can also examine properties other than the energy using ab initio methods. These properties depend on the electronic structure of the system. For example, details of the charge distribution can be used to describe a system as either covalently or ionically bonded, depending on the density of charge between atomic centers. Although the classification of a system as covalent or ionic using charge distribution is an oversimplification, such qualitative ideas about the nature of the interactions (in particular whether a given interaction is "long ranged" or "short ranged") play an important role in modelling transport properties of silicates. Secondly, the x-ray spectra of many crystalline and glassy materials have been determined. The interpretation of these spectra in terms of relative differences of energy eigenvalues provides another touchstone for modellers. Furthermore, ab initio calculations can be used to check the validity of the two-body interaction assumption used in deriving the empirical potential functions used in Chapter 3. A direct calculation of interaction energy as a function of geometry (including dispersion forces) permits a straightforward determination of the magnitudes of many-body contributions.

The generation of interaction energies as a function of geometry for a system involves several choices (Table 12). The reference state is the state of the system which determines the energy zero (see Equation 2.8). In thermodynamics this state is entirely arbitrary. However, due to approximations in the Hartree-Fock self-consistent-field (SCF) method, in practice the reference state is not arbitrary and is in fact quite important (Carsky, 1980). The SCF equations assume each of the electrons in a system move in a coulombic field generated by the nuclei and the time averaged positions of the other electrons. In reality the electron motions are highly correlated. This correlation energy can be quite large. When electron pairs are not conserved in transfer from one state to another, the correlation energy is not conserved either, and the resulting error can be larger than the difference in the energies of the states. Using closed-shell ions as the reference state for calculations on cation-oxygen cluster approximately conserves correlation energy, while using neutral atoms as the reference state for these clusters requires rupture of electron pairs resulting in a large correlation error.

At the present, most ab initio wavefunctions are linear combinations of atomic orbitals (LCAO's). The atomic orbitals are chosen to minimize the energy of isolated atoms or ions. Using the variation principle, these minimum energy wavefunctions are the best approximation to the real electronic charge distribution under the initial assumptions. The initial assumptions, i.e. the number of

Table 12

Choices for starting *ab initio* calculations
1. Choose a reference state
2. Choose a basis set
3. Choose clusters
4. Choose cluster geometries

functions, and their mathematical form, as well as the constants adjusted to minimize the energy comprise the basis set. Of particular importance is the size of the basis set, i.e. how many orbital exponents are used to describe the atomic charge distribution. Larger basis sets contain more orbitals, are more flexible, and possibly allow better description of the charge distribution in a molecular environment. The spurious lowering of the energy of a cluster relative to the energies of the isolated constituents is called counterpoise error, and is roughly inversely proportional to basis set size (Carsky, 1980). However the computing time is proportional to the fourth power of the number of orbital exponents.

The choice of which clusters to consider is perhaps the most difficult problem of all. Severe limitations are placed on the number of atomic centers and basis functions permitted in a computation due to storage requirements. Computing time is also an important limiting factor. The ideal cluster is large enough to contain all of the significant interactions in a crystal or liquid, yet still act as an energetically independent unit. Lastly, the number of geometries that can be examined for a given cluster is also limited by available computer time.

Basis Sets

I used five different basis sets for the calculations described later in this chapter (Carsky, 1980 contains a discussion of the mathematics of different types of basis sets). The first four

basis sets, taken from the literature, are based on fits of three gaussian functions to a single Slater-type orbital (STO) and denoted STO-3G. The first basis set (STO-3G; Hehre et al., 1969) has no d orbitals. The second basis set (STO-3G*; Pople et al., 1978) has a single d orbital on each silicon and magnesium center. The third basis set (STO-3G**; Pople et al., 1978) has a single d orbital on each silicon, magnesium, and oxygen center. These three basis sets have one exponent for every orbital. The fourth basis set, also taken from the literature (STO-3G DZ; Clementi, 1964) has no d orbitals, but has two functions to describe each orbital, and is termed a double zeta basis set. These four standard basis sets were all optimised for neutral atoms and are all imbalanced in that they have different numbers of orbital exponents for different atoms: (1s,2sp) for oxygen, and (1s,2sp,3sp) for Mg, Al, and Si. Orbital exponents for these basis sets can be found in the above mentioned references.

To compare with these four standard basis sets, I developed a small, balanced, highly optimized basis set. The basis sets for O, Mg, Al, and Si each consist of three STO's. The inner orbital function (the 1s function) is approximated by three gaussian functions, and the valance (2sp and 3sp) functions are approximated by three gaussian functions and one gaussian function respectively. This basis set is described as a 3-31G split valance basis set. Since the reference state was chosen to be ions at infinity, I optimized the basis set exponents for the individual closed-shell ions, using the

variation theorem. The orbital exponents for the 3-31G basis set developed in this study are listed in Table 13.

Silicon-Oxygen Clusters

The silicon-oxygen clusters are designed to simulate the properties of the polymorphs of SiO_2. The fundamental unit of these structures is the SiO_4^{4-} tetrahedron (except for stishovite, in which oxygen is six fold coordinated with silicon). The closed-shell unit carries the charge of -4, and the ground state is a singlet.

The first calculation is for the SiO_4^{4-} cluster with tetrahedral geometry: the Si-O distances are all 1.613 angstroms, the separation observed experimentally in quartz at 298 ^{o}K. Table 14 contains the energies, binding energies, and charges on each of the centers as calculated using each of the five basis sets. The energy eigenvalues differences from each of the calculations are compared with experimental x-ray spectra in Table 15. From an examination of the energies, and considering the variational theorem, the STO-3G DZ basis set can be seen to give the best wavefunction for the system, and the STO-3G set the worst. However, the STO basis sets all give binding energies that are too negative. (-2.19286E-10, obtained by dividing the binding energy of quartz, Table 5, by Avagadro's number.) Because the STO basis sets are optimised for neutrals, and are unbalanced (both factors in increasing counterpoise error) they are not useful for calculating binding energies. The 3-31G basis set is the only basis set examined that is useful in predicting binding energies.

Table 13

The 3-31G Basis Set

Ion	orbital exponent 1s	2sp	3sp
O^{2-}	7.69	1.91	0.89
Mg^{2+}	11.68	3.85	1.45
Al^{3+}	12.68	4.33	1.64
Si^{4+}	13.66	4.82	1.85

Table 14

Results of ab initio calculations for SiO_4^{4-}

Basis set	Energy (a.u.)	Binding energy (ergs)	q_{Si}^a	q_O^b
STO-3G	-578.48791	-2.75131×10^{-10}	0.601	-1.150
STO-3G*	-578.91056	-2.87642×10^{-10}	-0.137	-0.966
STO-3G**	-578.91580	-3.15558×10^{-10}	-0.126	-0.968
STO-3G DZ	-582.89817	-2.56103×10^{-10}	1.413	-1.353
3-31G	-579.25498	-2.13356×10^{-10}	3.455	-1.864

a. Charge on silicon.

b. Charge on oxygen.

Table 15

Relative orbital energies (eV) for SiO_4^{4-}

MO[c]	STO-3G*	STO-3G DZ	3-31G	Xα[a]	exp.[b] (SiO_2)
$1t_1$	0	0	0	0	0
1e	-0.8	-1.4	-1.3	-1.2	-1.9
$5t_2$	-2.2	-1.6	-1.8	-1.2	-1.9
$4t_2$	-4.5	-4.0	-3.7	-3.2	-4.8
$5a_1$	-7.1	-6.2	-5.7	-7.4	-7.8
$3t_2$	-22.9	-21.3	-23.0	-14.5	-18.4
$4a_1$	-24.7	-23.3	-24.7	-17.4	-20.8

a. Xα SCF calculation, Tossell (1975).

b. X-ray photoelectron spectrum of amorphous silica, DiStefano and Eastman (1971).

c. Molecular orbital.

The charges on each center are determined by a division of the cluster into "spheres of influence" about each center (the Mulliken population analysis, Mulliken, 1955). This procedure works well for core electrons that are strongly bound to a center, but the valance electron distribution is more diffuse, and its partitioning is rather arbitrary. In any case, it seems evident that the balanced 3-31G basis set calculation shows the Si-O bond is largely ionic. This result is confirmed by the STO-3G DZ calculation which partially accounts for lack of balance by its large size.

The results for the relative energy eigenvalue differences are rather inconclusive. All of the basis sets match the correct order of the energy levels. Qualitatively they are all as good as the $X\alpha$ technique (Tossell, 1975) at predicting the amorphous silica X-ray photoelectron spectrum. The quantitative differences could be due to the nature of the fragment used to represent amorphous silica, or to assumptions basic to all SCF quantum mechanical methods.

The next calculation is a geometry variation of the tetrahedron. The Si-O distance has been varied from 1.59 to 1.68 angstroms. The internal energy of β-quartz can be calculated using lattice sums and the repulsive energy from the quantum calculations. The repulsive energy as a function of distance for the cluster is presented in Figure 4 for the 3-31G basis sets, as well as for the empirical potential function developed in Chapter 3. The STO-3G potential, not shown in Figure 4 for clarity, has a minimum at 1.59 angstroms, and is much steeper than either the 3-31G or the empirical potential function.

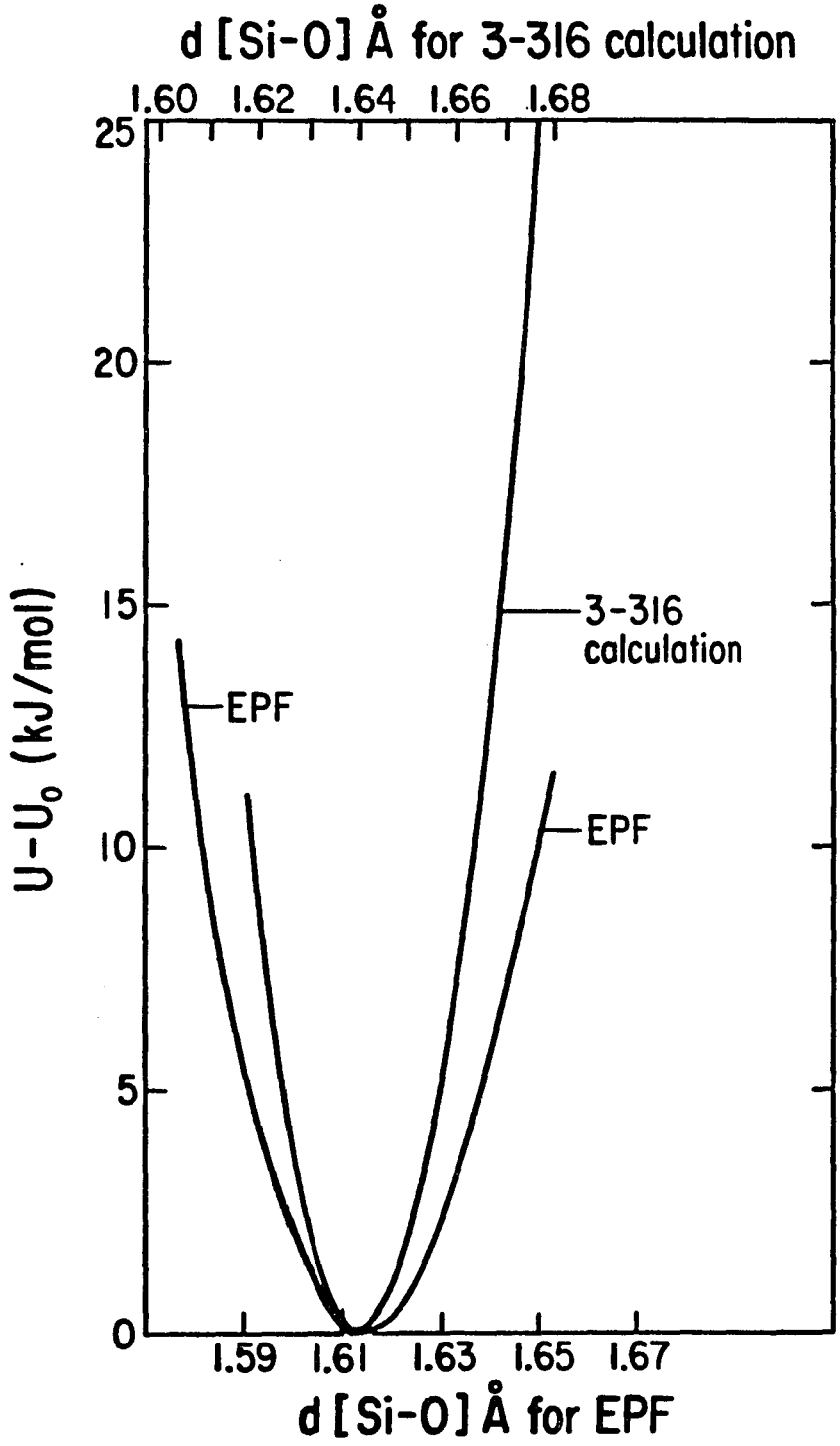

Figure 4. Geometry Variation of the SiO_4^{4-} Tetrahedron. -- The STO-3G potential is not shown here for clarity and is much steeper with a minimum at 1.59 angstroms.

As mentioned above, the absolute value of the minimum for the STO-3G potential function is 35 percent too negative. Only the 3-31G basis set is adequate for calculation of the binding energy with respect to geometry. The minimum energy distance is found to be 1.64 angstroms, compared to 1.613 angstroms in quartz. This difference could be due to non-independence of the tetrahedral units.

In order to test the independence of the tetrahedral units, two additional clusters have been examined using the 3-31G basis set: $Si_2O_7^{6-}$ and H_4SiO_4. In both of these clusters the electronic charge is distributed over more atomic centers, more nearly approximating the environment in condensed phases. The results of these calculations are in Tables 16 and 17. From examining the binding energies, apparently the tetrahedral units in the bitetrahedra are independent energetically to a good approximation, as the binding energies for the bitetrahedra almost exactly twice the binding energies calculated for a single tetrahedron (Table 14). The binding energies for the H_4SiO_4 molecule are not shown because the reference state energy is unknown. Note that even when the electronic charge has more atomic centers to cover, the bonding appears essentially ionic from the 3-31G calculated atomic charges.

In order to examine the independence of the tetrahedral units in terms of geometry, several different geometries were examined. In the first calculation, the Si-O distance only was varied (using 140 degrees as the intertetrahedral angle) and the minimum energy was found to be at 1.625 angstroms. Secondly, the dihedral angle was

Table 16

Results of ab initio calculations for $Si_2O_7^{6-}$ and H_4SiO_4

Basis set	Cluster	Energy (a.u.)	Binding Energy (ergs)	q_{si}	q_{br-O}	q_{nbr-O}
STO-3G*	$Si_2O_7^{6-}$	-1084.87301	-5.84898×10^{-10}	0.053	-0.570	-0.923
3-31G	$Si_2O_7^{6-}$	-1085.12243	-4.22919×10^{-10}	3.478	-1.951	-1.833
STO-3G*	H_4SiO_4	-583.51417	-	0.965	-0.477	-
3-31G	H_4SiO_4	-582.60487	-	3.540	-1.471	-

Table 17

Relative orbital energies (eV) for H_4SiO_4

MO[a]	STO-3G*	3-31G	exp[b] (SiO_2)
$1t_1$	0	0	0
1e	-1.8	-1.4	-1.9
$5t_2$	-1.9	-1.5	-1.9
$4t_2$	-7.6	-7.5	-4.8
$5a_1$	-10.5	-10.1	-7.8
$3t_2$	-23.7	-23.8	-18.4
$4a_1$	-24.9	-24.9	-20.8

a. Molecular orbital.

b. X-ray photoelectron spectrum of amorphous silica, DiStefano and Eastman (1971).

varied from staggered to eclipsed and the staggered configuration was found to have the lowest energy. Lastly, keeping the Si-O distance at 1.613 angstroms, and the dihedral angle at 60 degrees the intertetrahedral angle was varied from 180 degrees to 130 degrees. Considering the electronic and nuclear repulsion energies only, the 180 degree configuration had the lowest energy. These results are all similar to earlier calculations on the bitetrahedra (Zupan and Buh, 1976) and suggest that with the possible exception of the Si-O distance, the tetrahedral units in quartz are highly independent, and thus that many-body interactions are fairly unimportant in determining the equilibrium geometry.

Magnesium-Oxygen Clusters

The magnesium-oxygen clusters are designed to simulate the properties of periclase and magnesium in solution with silica. Magnesium is found in both four and six fold coordination with oxygen in silicate materials. The clusters studied are MgO_6^{10-} and MgO_4^{6-}. Both clusters are singlets in the ground state.

Table 18 contains the results of the calculations using the 3-31G basis set for energies, binding energies, and charges for the two magnesium-oxygen clusters. The charges indicate a fairly high degree of ionicity in the magnesium-oxygen interaction. The relative orbital energies for MgO_4^{6-} are listed in Table 19, along with the results of the X calculation by Tossell (1975). The energy differences

Table 18

Results of ab inito calculations for MgO_6^{10-} and MgO_4^{6-} (3-31G basis set)

	MgO_6^{10-}	MgO_4^{6-}
Energy (a.u.)	-630.90427	-489.00564
Binding energy (ergs)	-1.75684×10^{-10}	-9.33167×10^{-10}
q_{Mg}	1.969	1.909
q_O	-1.995	-1.977

Table 19

Relative orbital energies (eV) for MgO_4^{6-}

MO[b]	3-31G	Xα[a]
$5t_2$	0.3	0.2
$1t_1$	0	0
1e	-0.3	-0.9
$4t_2$	-0.7	-1.3
$5a_1$	-1.5	-1.6
$3t_2$	-20.5	-14.5
$4a_1$	-20.6	-14.7

a. Xα SCF calculation, (Tossell, 1975).

b. Molecular orbital.

qualitatively match the Xα calculation, although there is no photoelectron spectrum available for four fold coordinated magnesium.

Aluminum-Oxygen Clusters

Aluminum is also found in four and six fold coordination with oxygen in aluminates and silicates. The clusters chosen for study are AlO_6^{9-} and AlO_4^{5-}. In the ground state both clusters are singlets.

Table 20 contains the results of the calculations with the 3-31G basis set for the energies, binding energies, and charges for the two aluminum-oxygen clusters. The charges on each center indicate that there is considerable long-range nature in the aluminum-oxygen interaction. Table 21 shows the relative orbital energies for AlO_4^{5-} are similar for the 3-31G calculation and the Xα calculation.

Summary of Calculations using the 3-31G Basis Set

A summary of the potential energy per bond and the equilibrium bond lengths for Si-O, Al-O, and Mg-O bonds is given in Table 22. Given these results, and the qualitative similarities of the relative energy levels to experimental values and independent calculations, the 3-31G basis set can be used to describe the electronic structure of Mg-, Al-, and Si-oxygen clusters. I have drawn several specific conclusions:

1) The interactions between Mg, Al, and Si centers and oxygen centers is highly ionic. Previous ab initio calculations using STO basis sets were unable to address this question due to their unbalanced nature. Given equal flexibility of basis

Table 20

Results of ab inito calculations for AlO_6^{9-} and AlO_4^{5-} (3-31G basis set)

	AlO_4^{9-}	AlO_4^{5-}
Energy (a.u.)	-674.31844	-531.93045
Binding energy (ergs)	-6.1384×10^{-11}	-1.02296×10^{-10}
q_{Al}	2.809	2.742
q_O	-1.968	-1.936

Table 21

Relative orbital energies (eV) for AlO_4^{5-}

MO[b]	3-31G	Xα[a]
$1t_1$	0	0
$5t_2$	-0.5	-0.7
1e	-0.9	-1.2
$4t_2$	-1.9	-2.4
$5a_1$	-3.5	-5.6
$3t_2$	-13.1	-14.1
$4a_1$	-21.7	-16.0

a. Xα SCF calculation, (Tossell, 1975).

b. Molecular orbital.

Table 22

Summary of results of ab initio calculations (3-31G)

		calc.	exp.[a]
Si-O	bond energy (ergs)	-1.001×10^{-10}	-1.001×10^{-10}
Al-O	bond energy (ergs)	-7.129×10^{-11}	-7.076×10^{-11}
Mg-O	bond energy (ergs)	-4.273×10^{-11}	-4.164×10^{-11}
Si-O	bond distance (Å)	1.64	1.613
Al-O	bond distance (Å)	1.90	1.92
Mg-O	bond distance (Å)	2.13	2.11

a. Obtained from the binding energies in Table 5.

sets on each center, the electronic charge distribution is highly ionic. This implies long-ranged forces must be important in silicates.

2) With the possible exception of the Si-O bond length, in silicon-oxygen clusters the tetrahedral units are highly independent with respect to binding energy and geometry. The two-body approximation for the MAS system potential functions seems adequate.

3) Although the 3-31G calculated binding energies are fairly close to the experimental values, for magnesium in particular, the differences between calculation and experiment are on the order of tens of kilojoules. A much larger basis set would be needed to reduce this error. Given the present limitations on computer storage and time, the calculation from first principles of precise properties of silicate materials is not practical.

CHAPTER 5

GENERAL DISCUSSION AND FUTURE WORK

In the previous two chapters I have shown that a model which contains coulombic (i.e. long range) interactions is quantitatively consistent with the equilibrium properties of materials in the MAS system. In this chapter I will present a general model for the structure of silicates based on the results described previously. Other interaction laws have been proposed for silicates, in particular a model in which short-ranged interactions determine the properties of the materials and long-ranged interactions are not present. I will show that these short-ranged interactions models are consistent with, and can be derived from, long-ranged interaction models. Lastly, the approximations in the self-consistent-field Hartree-Fock ab initio method limit the usefulness of this method for determining interaction laws from first principles. I will address this subject also in this chapter.

A General Model for the Structure of Silicates

Many models to explain the equilibrium properties of various silicate systems have been advanced (see Chapter 2 for a discusssion of several of these models). None have been successful in explaining the behavior of silicates seen over large compositional ranges. Some of the more basic phenomena are:

1) Coordination Behavior Silicon and titanium are always found in tetrahedral coordination with oxygen (at one atmosphere) in silicate solids and liquids. Aluminum is found in four and six fold coordination in silicate solids, and in a mixture of coordination numbers in silicate liquids (McMillan, 1981). The remaining cations, magnesium, iron, calcium, sodium, and potassium are only found in higher coordination numbers in silicates.

2) Electrical Conductivity Charge transfer in silicate liquids is accomplished primarily by tranfer of ions. The transfer is also unipolar, with mobile cations (magnesium, calcium, iron, potassium, and sodium) and fixed anions. This suggests that the anions, i.e. oxygen in volatile free melts, define a structure in which the charge carrying cations fit in as best they can. None of the charge transfer is due to tetrahedrally coordinated species, suggesting that these species are also part of the defining structure.

3) Volume Relations The volumes of mixing in binary $MO-SiO_2$ melts show negative deviations from ideality. This further suggests that cations break down the silica framework and occupy sites in that framework.

4) Polymerized structure Silicate solids and liquids become more polymerized with the addition of silica. In solids, the progression is from isolated tetrahedra to chains to double chains to sheets to a framework structure. In liquids the

progression is similar, although liquids are in general polydisperse in the polymeric species they contain.

6) Liquid Immiscibility At high silica contents in binary MO-silica systems there is a region with positive free energies of mixing.

The model developed in this dissertation is the only model which has quantitatively explained these six types of behavior. In this model, the simplest structural components are the cations and anions. These particles interact through coulombic dispersion, and repulsive forces. In general, silicon is found to have the strongest affinity for oxygen, and if enough oxygen is available (i.e. at least two times the number of atoms of silicon) as is always the case in naturally occuring silicate systems, silicon is able to surround itself with four oxygen anions, and these tetrahedra join only at the apices. Edge and face joining are unfavorable energetically due to the electrostatic repulsion of the silicon ions at the center of the tetrahedra. Depending on the amount of oxygen available and the number of other cations present (which because of their large size tend to break up a polymerized network) the SiO_4^{4-} tetrahedra will polymerize. This polymerization is energetically favorable because an extra oxygen anion is feed to interact with other cations.

Aluminum has the next highest affinity for oxygen, so its behavior depends on the amount of oxygen present. In most silicates there is enough oxygen present so that some of the aluminum can be in the most energetically favorable state, which is tetrahedrally

coordinated with oxygen (if enough oxygen is available to satisfy all of the aluminum, the other cations then compete for the remainder according to their affinity for oxygen). The rest of the aluminum, along with the other lower charged cations, sit in larger sites in the framework. These sites are lower energy configurations, but must be created because of local charge balance and packing considerations. Liquid immiscibility is explained in this model as unmixing between high silica neutral framework structures and lower silica (i.e. higher cation) charged chain structures. In the ion competition formalism, the structural properties of silicates are seen to arise from differences in the affinity for oxygen of the cations, local charge balance, and packing considerations.

The Nature of the Interparticle Forces in Silicates

In finding the empirical potential functions (Chapter 3) which describe the interaction of the particles in silicate systems, a form incorporating ionic (i.e. long-ranged) interactions was used. Other forms involving short-ranged attractive forces have been used to describe the properties of silicates. The attractive forces in these models vary as inverse six and higher powers of the separation. The model described above is qualitatively independent of which form is used for the attractive interaction: what is important is the depth of the potential wells of each of the cations with oxygen. However the question of which type of force law to use is an important one for quantitative purposes, as well as for describing transport properties.

The electrical conductivity data argue strongly that ionic species exist in silicate liquids. Empirical rules for trace element distribution between crystals and liquids also suggest that the species in crystals are also ionic. Furthermore, as seen in Chapter 4, the electron distribution calculated using a balanced basis set indicates that in cation-oxygen interactions, the centers are highly charged. The presence of charged species in silicate materials must be considered fairly well established.

Quantum Mechanics

The self-consistent-field Hartree-Fock method used in this work for examing the properties of small silicate clusters has some general deficiencies for examining the interactions in silicate materials. These deficiencies arise from the assumptions basic to the method and from limitations of computer time and storage.

The SCF approximation is that each of the electrons in a cluster move in a coulombic field which is generated by the nuclei and the average positions of the other electrons. However, the electron motions are highly correlated. As discussed in Chapter 4, this correlation energy is fairly large, and cannot be ignored when calculating binding energies. Even when ions separated at infinity are used as the reference state, which approximately conserves correlation energy, the variation of energy with distance is affected. In order to obtain thermodynamically accurate potentials and force constants correction must be made for this effect.

The second approximation is the description of the electron distribution in ions and clusters in terms of basis functions. Since the number of two electron integrals grows as the fourth power of the number of basis functions, accurate description of the electron distribution in terms of a small number of basis functions optimized for each cluster and geometry would be desirable. Unfortunately this optimization, using the variational principle is also a time consuming process. The linear combination of atomic orbitals approach attempts to circumvent this problem by optimizing basis sets for individual ions, and describing the charge distribution as a linear combination of these optimized functions. Unfortunately, there is little to suggest that the actual charge distribution in a molecular cluster is best approximated using this method.

The basis set problem also interacts with the next problem, the choice of which clusters best represent the extended system. The larger and more flexible the basis set, the smaller the clusters must be. On the other hand, if very small basis sets are employed then the results for the larger clusters are unreliable. Given present limits on computer time and storage, the 3-31G basis set described earlier is among the largest practical for examining clusters such as $Si_2O_7^{6-}$, AlO_6^{9-}, and MgO_6^{10-}. Furthermore, the number of geometries that can be studied for each cluster is also limited. Future work in this area must correct these deficiencies if substantial progress is to be made.

LIST OF REFERENCES

Adams D. J. and McDonald I. R. (1974) Rigid ion models of the interionic potential in the alkali halides. Jour. Phys. C: Solid State Phys. 7, 2761-275.

Baes C. F. Jr (1970) A polymer model for BeF_2 and SiO_2 melts. J. Solid State Chem. 1, 159-169.

Barron L. M (1972) Thermodynamic multicomponent silicate equilibrium phase calculations. Am. Mineral. 57, 809-823.

Bockris J. O'M. and Lowe D. C. (1954) Viscosity and the structure of molten silicates. Proc. Royal Soc. 226A, 423-435.

Bockris J. O'M. and Mellors G. W. (1956) Electric conductance in liquid lead silicates and borates. J. Phys. Chem. 60, 299-310.

Bockris J. O'M., Kitchener J. A., Ignatowicz S. and Tomlinson J. W. (1952a) Electric conductance in liquid silicates. Trans. Farad. Soc. 48, 75-91.

Bockris J. O'M., Kitchener J. A. and Davies A. E. (1952b) Electric transport in liquid silicates. Trans. Farad. Soc. 48, 536-548.

Bockris J. O'M., Mackenzie J. D. and Kitchener J. A. (1955) Viscous flow in silica and binary liquid silicates. Trans. Farad. Soc. 51, 1734-1748.

Bockris J. O'M., Tomlinson J. W. and White J. L. (1956) The structure of liquid silicates: partial molar volumes and expansivities. Trans. Faraday Soc. 152, 299-310.

Born M. and Mayer J. E. (1932) Zur gittertheorie der ionenkristalle. Z. Physik 75, 1-18.

Bottinga Y. and Richet P. (1978) Thermodynamis of liquid silicates, a preliminary report. Earth Planet. Sci. Let. 40, 382-400.

Bottinga Y. and Weill D. F. (1972) The viscosity of magmatic silicate liquids: a model for calculation. Am. Jour. Sci. 272, 438-475.

Bowen N. L. (1928) The evolution of the igneous rocks. New York, Dover Press.

Brush S. G, Sahlin H. L. and Teller E. (1966) A Monte Carlo study of a one-component plasma. J. Chem. Phys. 45, 2102-2118.

Carsky P. (1980) Ab initio calculations: methods and applications in chemistry, New York, Springer-Verlag.

Clark S. P. Jr (1966) Handbook of physical constants, New York, Geol. Soc. Am.

Clementi E. (1964) Simple basis set for molecular wavefunctions containing first- and second-row atoms. J. Chem. Phys. 40, 1944-1945.

De Jong B. H. W. S. and Brown G. E. Jr (1980) Polymerization of silicate and aluminate tetrahedra in glasses, melts, and aqueous solutions- I. Electronic structure of $H_6Si_2O_7$, H_6AlSiO_7, and $H_6Al_2O_7$. Geochim. Cosmochim Acta 44, 491-511.

DiStefano T. H. and Eastman D. E. (1971) Photoemission measurements of the valance levels of amorphous SiO_2. Phys. Rev. Lett. 27, 1560-1562.

Dowty E. (1980) Crystal-chemical factors affecting the modility of ions in minerals. Am. Mineral. 65, 174-182.

Drake M. J. (1976) Plagioclase-melt equilibria. Geochim. Cosmochim. Acta 40, 457-465.

Eitel W. (1954) The physical chemistry of the silicates, Chicago, Univ. Chi. Press.

Ewald P. P. (1921) Die berechnung optischer and elektrostatischer gitterpotentiale. Ann. Phys. 64, 253-287.

Fraser D. G. (1977) Thermodynamic properties of silicate melts. Thermodynamics for Geologists (ed. D. G. Fraser), Chapter 15, Reidel.

Gaskell D. R. and Ward R. G. (1967) Density of iron oxide-silica melts. Trans. Met. Soc. 239, 249-252.

Gotz J. and Masson C. R. (1971) Trimethylsilyl derivatives for the study of silicate structures. Part II. Orthosilicate, pyrosilicate, and ring structure. J. Chem. Soc. A 686-688.

Hehre W. J., Stewart R. F. and Pople J. A. (1969) Self consistent molecular-orbital methods. I. Use of Gaussian expansions of Slater-type orbitals. J. Chem. Phys. 51, 2657-2664.

Henderson J., Hudson R. G., Ward R. G. and Derge W. (1961) Density of liquid iron silicates. Trans. Met. Soc. 221, 807-811.

Hirschfelder J. O., Curtiss C. F. and Bird R. B. (1954) Molecular theory of gases and liquids, Chicago, Wiley.

Hostetler C. J. and Drake M. J. (1980) Predicting major element mineral/melt equilibria: a statistical approach. J. Geophys. Res. 85, 3789-3796.

Huggins M. L. (1937) Lattice energies, equilibrium distances, compressibilities, and characteristic frequencies of alkali-halide crystals. J. Chem. Phys. 5, 143-148.

Huggins M. L. (1947) Errata: Lattice energies, equilibrium distances, compressibilities, and characteristic frequencies of alkali-halide crystals. J. Chem. Phys. 15, 212.

Huggins M. L. and Mayer J. E. (1933) Interatomic distances in the crystals of the alkali halides. J. Chem. Phys. 1, 643-646.

JANAF (1971) Thermochemical tables, Nat. Bur. Stan. Pub. 37.

Johnson Q. C. and Templeton D. H. (1961) Madelung constants for several structures. J. Chem. Phys. 34, 2004-207.

Ladd M. F. C. (1974) van der Waals potentials and crystal energies of ionic compounds. J. Chem. Phys. 60, 1954-1957.

Lantelme F., Turg P., Quentrec B. and Lewis J. W. E. (1974) Application of the molecular dynamics method to a liquid system with long range forces (molten NaCl). Mol. Phys. 28, 1537-1549.

Lentz C. W. (1963) Silicate minerals as a source of trimethylsilyl silicates and silicate structure analysis of sodium silicate solutions. Inorg. Chem. 3, 574-579.

Longhi J., Walker D. and Hays J. F. (1978) The distribution of Fe and Mg between olivine and lunar basaltic liquids. Geochim. Cosmochim. Acta 42, 1545-1558.

Masson C. R. (1968) Ionic equilibria in liquid silicates. J. Am. Ceram. Soc. 51, 134-143.

Masson C. R., Smith I. B., and Whiteway S. G. (1970) Activities and ionic distributions in liquid silicates: application of polymer theory. Can. J. Chem. 48, 1456-1464.

McMillan P. (1981) A structural study of aluminosilicate glasses by Raman spectroscopy. Ph. D. Dissertation, Arizona State University.

McMillan P. and Piriou B. (1982) The structures and vibrational spectra of crystals and glasses in the silica-alumina system. J. Non-Cryst. Solids, in press.

Mulliken R. E. (1955) Electronic population analysis on LCAO-MO molecular wavefunctions. I. J. Chem. Phys. 23, 1833-1840.

Navrotsky A., Peraudeau G., McMillan P. and Coutures J. (1982) A thermochemical study of glasses and crystals along the joins silica-calcium aluminate and silica-sodium aluminate. Geochim. Cosmochim. Acta, in press.

Nesbitt H. W. and Fleet M. E. (1981) An ion-association model for PbO-SiO_2 melts: interpretations of thermochemical, conductivity, and density data. Geochim. Cosmochim. Acta 45, 235-244.

Nielsen R. L. and Drake M. J. (1979) Pyroxene-melt equilibria. Geochim. Cosmochim. Acta 43, 1259-1272.

Papike J. J. and Cameron M. (1976) Crystal chemistry of silicate minerals of geophysical interest. Revs. Geophys. Space Phys. 14, 37-80.

Pauling L. (1928) The influence of relative ionic sizes on the properties of ionic compounds. J. Am. Chem. Soc. 50, 1036-1045.

Philpotts J. A. (1978) The law of constant rejection. Geochim. Cosmochim. Acta 42, 909-920.

Pople J. A., Binkley J. S., Whitehead R. A., Harihan P.C. and Seiger R. (1978) Gaussian-76: An ab initio molecular orbital calculation. Quantum Chemistry Program Exchange 11, 368.

Riebling E. F. (1964) Structure of magnesium aluminosilicate liquids at 1700°C. Can. J. Chem. 42, 2811-2821.

Riebling E. F. (1966) Structure of sodium aluminosilicate melts containing at least 50 mol % SiO_2 at 1500°C. J. Chem. Phys. 44, 2857-2865.

Robie R. A., Hemingway B. S. and Fisher J. R. (1978) Thermodynamic propeties of minerals and related substances at 298.15° K and 1 bar pressure and at higher temperatures. U. S. Geol. Survey Bull. 1452.

Roeder P. L. (1974) Activity of iron and olivine solubility basaltic liquids. Earth Plan. Sci. Let. 23, 397-410.

Roeder P. L. and Emslie R. F. (1970) Olivine-liquid equilibrium. Contrib. Mineral. Petrol. 29, 275-289.

Segers L., Fontana A. and Winand R. (1978) Conductivities electriques de melanges de silicates fondus du systeme Cao-SiO_2-MnO. Electrochimica Acta 23, 1281-1286.

Seifert F., Mysen B. O. and Virgo D. (1982) Three dimensional network melt structure in the systems SiO_2-$CaAl_2O_4$ and SiO_2-$MgAl_2O_4$. Amer. Mineral., in press.

Swaminathan S., Whitehead R. J., Guth E. and Beveridge D. L. (1977) A heuristic intermolecular potential function for formaldehyde-water based on ab initio molecular orbital calculations. J. Am. Chem. Soc. 99, 7817-7822.

Tomlinson J. W., Heynes M. S. R., and Bockris J. O'M. (1958) The structure of liquid silicates. Part 2. Molar volumes and expansivities. Trans. Farad. Soc. 54, 1822-1833.

Tosi M. P. (1964) Cohesion of ionic solids in the Born model. Solid State Phys. 16, 1-120.

Tosi M. P. and Fumi F. P. (1964) Ionic sizes and Born repulsive parameters in the NaCl-type alkali halies- II The generalized Huggins-Mayer form. J. Phys. Chem. Sol. 25, 45-52.

Tossell J. A. (1975) The electronic structures of silicon, aluminum, and magnesium in tetrahedral coordination with oxygen from SCF-X MO calculations. J. Am. Chem Soc. 97, 4840-4844.

Tossell J. A. (1980) Calculation of bond distances and heats of formation for BeO, MgO, SiO_2, TiO_2, FeO and ZnO using the ionic model. Am. Mineral. 63, 163-173.

Wackman P. H., Hirthe W. M. and Frounfelker R. E. (1967) The cohesive energy of TiO_2 (Rutile). J. Phys. Chem. Solids 28, 1525-1531.

Waseda Y. (1980) The structure of non-crystalline materials. New York, McGraw-Hill.

Wood W. W. (1968) Monte Carlo calculations for hard disks in the isothermal-isobaric ensemble. J. Chem. Phys. 48, 415-434.

Woodcock L. V. and Singer K. (1971) Thermodynamic and structural properties of liquid ionic salts obtained by Monte Carlo computation. Trans. Farad. Soc. 67, 12-29.

Zupan J. and Buh M. (1978) Ab initio calculation on the $(Si_2O_7)^{6-}$ bitetrahedra. J. Non-Cryst. Solids 27, 127-133.